Frequency-Dependent FDTD Modeling of Optically Controlled Dielectric Resonators

Ying Shen, *Student Member, IEEE,* Kent Nickerson, John Litva, *Senior Member, IEEE*

Abstract— **A theoretical analysis is carried out to describe the performance of optically controlled dielectric resonators. A previously developed frequency-dependent finite-difference time-domain formulation has been used to estimate the effect that solid state plasmas have on the resonant frequency of dielectric resonators. Optical generation of plasmas in contact with dielectric resonators is being considered here as a possible means of controlling the resonator's frequency. The effect that carrier diffusion and recombination-generation have on plasma permittivity and penetration depth are taken into account in this analyses.**

The results are compared with measurement and are shown to yield a quantitative estimate of the optically induced dielectric resonator frequency shift as a function of the illumination, properties of the plasma host semiconductor, and the properties of the dielectric resonator.

I. Introduction

Dielectric resonators (DR's) are a basic element in microwave integrated circuits. They have proven their usefulness in microwave band-reject and bandpass filters, slow-wave structures, frequency converters, diode and FET oscillators, as well as frequency-selective limiters [1]–[3]. They are also compatible with TEM-line, waveguide, and microstrip transmission line circuits [4], [5]. If one considers all of these applications, the DR's resonant frequency is obviously the most important of all its parameters, in terms of the control and adjustment that needs to be exercised once the device is in situ. One well-known tuning method incorporates the variable proximity of a metal plate adjusted by a screw [6], [7]. There are several mechanical shortcomings, however, associated with a tuning plate. These include temperature sensitivity, difficulty of incorporation in MMIC circuits and inherently slow tuning adjustment. An elegant nonmechanical substitute for the plate is an optically induced sheet of plasma on the surface of a slab of semiconductor. This new tuning element, discussed by Herczfeld *et al.* [8], defines a novel device called an optically controlled dielectric resonator (OCDR).

Interest in optical control of microwave devices and subsystems is growing rapidly [9]–[14] since it offers the potential advantages of very high bandwidth, inherently high dc and reverse isolation between control and RF signals, and compatibility with optical fiber links.

This paper describes the frequency-dependent finite-difference time-domain method's first reported application to modelling the performance of an OCDR. The two major effects of a constantly illuminated semiconductor plasma which must be analyzed are 1) the strong influence of carrier diffusion and recombination-generation processes on the dielectric constant and 2) the depth to which the plasma penetrates the device. Finally, the theoretical model is compared with available experimental results [8].

Manuscript received April 24, 1992; revised October 9, 1992. This work was supported by the Telecommunications Research Institute of Ontario.

The authors are with the Communications Research Laboratory, McMaster University, Hamilton, Ont. L8S 4K1, Canada.

IEEE Log Number 9208343.

II. Theory

A. Concept of the Optically Controlled Dielectric Resonator

Fig. 1(a) depicts a dielectric resonator with a slab of intrinsic semiconductor placed on top. Optical resonator tuning is realized when the slab is illuminated by light of a wavelength shorter than the semiconductor bandgap (e.g., about 880 nm for GaAs), thus forming a sheet of plasma on the illuminated semiconductor face. The light can be locally generated or supplied by an optical waveguide. The diameter and height of the dielectric resonator proper are selected so that the resonator supports a $TE_{01\delta}$ mode. The depth of injection for the optically iduced plasma is a fuction of the host semiconductor's optical absorption and the wavelength of the illumination [13]. Generally, shorter wavelengths suffer higher semiconductor absorption and hence a thinner region of injection.

For a sufficiently small plasma injection thickness, the final steady state plasma thickness is determined primarily by carrier diffusion and recombination. The plasma layer will have a higher microwave dielectric constant than the semiconductor host material. One then expects to see the resonant frequency increase with the plasma density, since the plasma acts like a conductive tuning plate. The magnitude of the frequency shift Δf as a function of the illumination intensity (and hence plasma density) depends on the resonator's material and geometric design. Deriving this relation theoretically is the object of this paper.

B. The Frequency-Dependent Finite-Difference Time-Domain Method

The finite-difference time-domain (FDTD) technique permits a fundamental electromagnetic analysis of volumes containing arbitrarily shaped dielectric and metal objects using differential forms of Maxwell's equations. First proposed by Yee in 1966 [15], FDTD simulation has been applied by many investigators to a wide range of electromagnetic problems. Extension of the FDTD method to frequency-

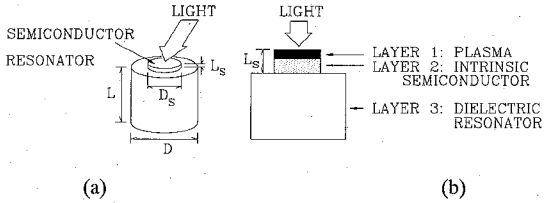

Fig. 1. (a) Optically controlled dielectric resonator schematic. (b) Definition of simulated layers.

dependent materials has, until recently, received relatively little attention. The most pertinent previous paper [16] is limited to one dimension without a FDTD context. The frequency-dependent FDTD, or $(FD)^2TD$, method was first presented by Luebbers *et al.* in 1990 [17], [18]. It allows explicit calculation of wide-band transient electromagnetic interactions with frequency dependent materials. This overcomes a serious limitation in current formulations of the FDTD method, which must specify the electromagnetic parameters ϵ, μ, and σ as constants. For this paper we assume that the plasma is linear, isotropic and is adequately described by a complex frequency dependent dielectric constant $\epsilon(w)$. Extension to the case of an anisotropic plasma should be possible.

The fundamental advantage of a frequency domain numerical analysis is that the electromagnetic parameters are constant at each frequency. In the time domain, all of the frequency domain permittivity information is Fourier transformed into a time domain susceptibility function. The formulation of the $(FD)^2TD$ method incorporates the necessary convolution into the traditional FDTD method. We assume the reader's familiarity with the basic Yee algorithm [15].

In the typical layered cylindrical OCDR structure of Fig. 1(b), the permittivity of the layer 1 plasma is frequency dependent, while that of layers 2 and 3 are frequency independent. The $(FD)^2TD$ algorithm is therefore applied only to layer 1. The resonator is assumed to support only $TE_{01\delta}$ modes for the simulation. Details of the FDTD algorithm applied to layers 2 and 3 are described in the authors' previous papers [6], [19], [20].

The time domain electric vector equation [17] is

$$\boldsymbol{D}(t) = \epsilon_\infty \epsilon_0 \boldsymbol{E}(t) + \epsilon_0 \int_0^t \boldsymbol{E}(t-\tau)\chi(\tau)\, d\tau \tag{1}$$

where ϵ_0 is the permittivity of free space, $\chi(\tau)$ is the electric susceptibility, and ϵ_∞ is the relative permittivity as $\omega \to \infty$. Here, we assume that $\epsilon_\infty = 1$ for all materials [17].

Using Yee's notation, the relationship between $\boldsymbol{D}$ and $\boldsymbol{E}$, for $t = n\Delta t$, is

$$D(t) \simeq D(n\Delta t) = D^n = \epsilon_\infty \epsilon_0 E^n + \epsilon_0 \int_0^{n\Delta t} E(n\Delta t - \tau)\chi(\tau)\, d\tau. \tag{2}$$

Using a central difference scheme [15], [17], [18], Yee's time differential form of Maxwell's equations [6] can be discretized to the following form:

$$\begin{aligned} E_g^{n+1}(i,j) &= \frac{\epsilon_\infty(i,j) + \Delta x_0(i,j)}{\epsilon_\infty(i,j) + x_0(i,j)} E_\theta^n(i,j) \\ &+ \frac{1}{\epsilon_\infty(i,j) + x_0(i,j)} \psi_\theta^n(i,j) \\ &+ \frac{\Delta t}{[\epsilon_\infty(i,j) + x_0(i,j)]\epsilon_0} \\ &\cdot \left\{ \left[\frac{H_r^{n+(1/2)}(i, j+\frac{1}{2}) - H_r^{n+(1/2)}(i, j-\frac{1}{2})}{\Delta z} \right] \right. \\ &\left. - \left[\frac{H_z^{n+(1/2)}(i+\frac{1}{2}, j) - H_z^{n+(1/2)}(i-\frac{1}{2}, j)}{\Delta r} \right] \right\} \end{aligned} \tag{3}$$

$$\begin{aligned} H_r^{n+(1/2)}\left(i, j+\frac{1}{2}\right) &= H_r^{n-(1/2)}\left(i, j+\frac{1}{2}\right) \\ &+ \frac{\Delta t}{\Delta z}\frac{1}{\mu}[E_\theta^n(i,j) - E_\theta^n(i,j-1)] \end{aligned} \tag{4}$$

$$\begin{aligned} H_z^{n+(1/2)}\left(i+\frac{1}{2}, j\right) &= H_z^n\left(i+\frac{1}{2}, j\right) \\ &- \frac{\Delta t}{\mu \Delta r r_{i+(1/2)}}[r_{i+1}E_\theta^n(i+1,j) - r_i E_\theta^n(i,j)] \end{aligned} \tag{5}$$

where

$$x_0(i,j) = \frac{w_p^2(i,j)}{v_c(i,j)}\Delta t - \left(\frac{w_p(i,j)}{v_c(i,j)}\right)^2 \cdot (1 - e^{-v_c(i,j)\Delta t}) \tag{6}$$

$$\Delta x_m(i,j) = -\left(\frac{\omega_p(i,j)}{v_c(i,j)}\right)^2 \cdot e^{-m v_c(i,j)\Delta t}(1 - e^{-v_c(i,j)\Delta t})^2 \tag{7}$$

$$\psi_\theta^n(i,j) = \sum_{m=1}^{n-1} E_\theta^{n-m}(i,j)\Delta x_m(i,j) \tag{8}$$

$$\psi_\theta^n(i,j) = E_\theta^{n-1}(i,j)\Delta x_1(i,j) + e^{-v_c(i,j)\Delta t}\psi_\theta^{n-1}(i,j) \tag{9}$$

and v_c is the collision frequency, ω_p is the plasma frequency (in rad $\cdot$ s^{-1}). The complex permittivity $\epsilon(\omega)$ for an isotropic plasma is given by [13], [17]

$$\epsilon(\omega) = \epsilon_0\left(\epsilon_L + \frac{\omega_p^2}{\omega(jv_c - \omega)}\right) \tag{10}$$

where ϵ_L is the dielectric constant of the plasma host including the contributions of bound charges.

C. Complex Permittivity of the Plasma Region

Due to contributions from free charges, the plasma layer differs from that of the remainder of the plasma host. For a classical electron-hole plasma, we expect the permittivity to

TABLE I
PLASMA FREQUENCY AND COLLISION TIME FOR DIFFERENT CARRIERS

i (i=1,2,3,4,5)	ω_{pi}	τ_i
1: intrinsic holes	$\frac{n_{p0}e^2}{\epsilon_0 m_p^*}$	τ_p
2: intrinsic electrons	$\frac{n_{e0}e^2}{\epsilon_0 m_e^*}$	τ_e
3: photoinduced electrons	$\frac{n_e e^2}{\epsilon_0 m_e^*}$	τ_e
4: photoinduced light holes	$\frac{P_l e^2}{\epsilon_0 m_{pl}^*}$	τ_p
5: photoinduced heavy holes	$\frac{P_h e^2}{\epsilon_0 m_{ph}^*}$	τ_p

follow the theoretical predictions of the Drude theory [13], [20], which defines a collision frequency $v_c = 1/\tau$ and a plasma frequency ω_p such that

$$\omega_p^2 = \frac{ne^2}{\epsilon_0 m^*} \tag{11}$$

where τ is the collision time, n is the plasma density, e is the electric charge, and m^* the carrier effective mass. Equation (10) can now be written as

$$\epsilon_r = \epsilon_L - \frac{\omega_p^2}{\omega^2 + v_c^2} - j\frac{v_c}{\omega}\frac{\omega_p^2}{\omega^2 + v_c^2}. \tag{12}$$

This shows that the difference between the plasma permittivity and that of the host depends on plasma density, the collision frequency of the plasma, and the frequency of the microwave signal. Substituting for ω_p and v_c, assuming an intrinsic host, and assuming high level injection conditions $(n_e = n_p)$, yields the following expansions for (12):

$$\frac{\omega_p^2}{\omega^2 + v_c^2} = \sum_{i=1}^{5} \frac{n_i e^2 \tau_i^2}{m_i^* \epsilon_0 (1 + \omega^2 \tau_i^2)} \tag{13}$$

$$\frac{v_c}{\omega}\frac{\omega_p^2}{\omega^2 + v^2} = \sum_{i=1}^{5} \frac{n_i e^2 \tau_i}{\omega m_i^* \epsilon_0 (1 + \omega^2 \tau_i^2)} \tag{14}$$

where $i = 1, 2, 3, 4, 5$, respectively, correspond to intrinsic holes, intrinsic electrons, photoinduced electrons, and photoinduced light and heavy holes. Table I gives ω_{pi} and τ_i for each of these cases.

Collision times for electrons and holes are

$$\tau_e = \frac{\mu_e m_e^*}{\epsilon}; \quad \tau_p = \frac{\mu_p m_p^*}{\epsilon} \tag{15}$$

where μ_e, μ_p are the respective electron and hole mobilities.

Combining the effects of illumination as described in (13)–(15) with (6) and (7) yields

$$x_0(i,j) = \sum_{i=1}^{5} \left[\frac{\omega_{pi}^2}{v_{ci}} \Delta t - \left(\frac{\omega_{pi}}{v_{ci}}\right)^2 (1 - e^{-v_{ci}\Delta t}) \right] \tag{16}$$

TABLE II
NUMERICAL PARAMETERS FOR Si AND GaAs AT $T = 300$ K

parameters	Si (T=300 K) [13]	GaAs (T=300 K) [23]-[25]
m_e^*	0.259 m_0	0.07 m_0
m_p^*	0.38 m_0	0.713 m_0
m_{pl}^*	0.16 m_0	0.12 m_0
m_{ph}^*	0.49 m_0	0.68 m_0
μ_e	1500 $cm^2/V.s$	8500 $cm^2/V.s$
μ_p	600 $cm^2/V.s$	400 $cm^2/V.s$
n_{p0}	10^{11} cm^{-3}	$1.1 * 10^7$ cm^{-3}
n_i	$1.18 * 10^{10}$ cm^{-3}	$2.25 * 10^6$ cm^{-3}
P_l	$0.14n_p$	$0.13n_p$
P_h	$0.86n_p$	$0.87n_p$
e	$1.6 * 10^{-19}$ coul	$1.6 * 10^{-19}$ coul
m_0	$9.11 * 10^{-31}$ kg	$9.11 * 10^{-31}$ kg
ϵ_L	11.8	10.9
E_g	1.12 eV	1.43 eV

$$\Delta x_m(i,j) = \sum_{i=1}^{5} \left[-\left(\frac{\omega_{pi}}{v_{ci}}\right)^2 e^{-mv_{ci}\Delta t}(1 - e^{-v_{ci}\Delta t})^2 \right] \tag{17}$$

D. Recombination-Generation Processes and Skin Depth in Plasma Host

The net steady-state recombination rate for an semiconductor illuminated strongly enough to support high level injection where $n_e = n_p \gg n_{p0}$ or n_{e0}, can be written [21], [22]

$$R_r = \frac{n_e}{\tau_p + \tau_e} \tag{18}$$

while the electron-hole generation rate is

$$G = \frac{P(1-R)}{E_g e A \delta} \tag{19}$$

where P is the input light power, R is the reflection coefficient at the air-semiconductor interface, E_g is the semiconductor bandgap, A is the area of the plasma (which is normally equal to the illuminated area), and δ is the $1/e$ illumination penetration depth. Note that the product $A\delta$ is the volume occupied by the plasma.

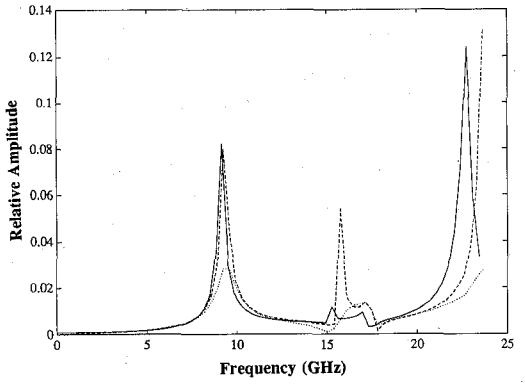

Fig. 2. Predicted $TE_{01\delta}$ mode resonant frequency shift for a X-band resonator ($\epsilon_r = 36$) versus plasma density for various plasma depths of 100, 200, and 400 μm in silicon.

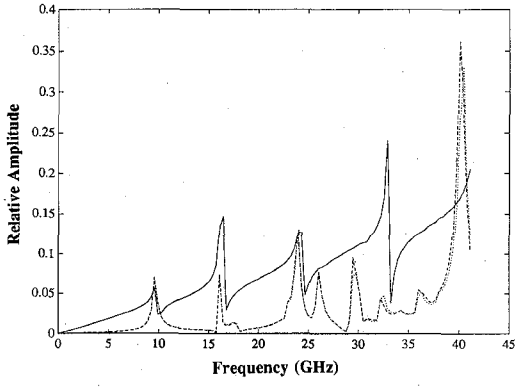

Fig. 3. Predicted $TE_{01\delta}$ mode resonant frequency shift for a Ka-band resonator ($\epsilon_r = 29.1$) versus plasma density for plasma depths of 100, 200, and 400 μm in GaAs.

Under equilibrium conditions, the recombination rate is equal to the generation rate. It follows, then, that the relationship between plasma density n_e and the input power P is

$$P = \frac{E_g e A \delta}{(\tau_p + \tau_e)(1 - R)} n_e. \tag{20}$$

III. Results

A. Theoretical Results

The simulated OCDR was subjected to a modeled abrupt electric field excitation so that many resonant modes were excited. A Fourier transform was then applied to the response to extract the resonant frequencies from the simulated results. Two types of OCDR's were considered: an X-band resonator tuned by a silicon (Si) semiconductor wafer; and a K-band resonator with a wafer of gallium arsenide (GaAs). Properties of the semiconductors are listed in Table II.

Fig. 2 shows the $TE_{01\delta}$ mode resonant frequency shift for an illuminated Si slab (with dimensions $D_s \times L_s = 1.76 \times 0.60\,\mathrm{mm}^2$) on an X-band ($f_0 = 10.92$ GHz) dielectric resonator ($D \times L = 5.46 \times 2.46\,\mathrm{mm}^2, \epsilon_r = 36$), as a function of plasma density for various thicknesses of the plasma layer. Figure 3 is a similar plot for the case of a GaAs tuning slab

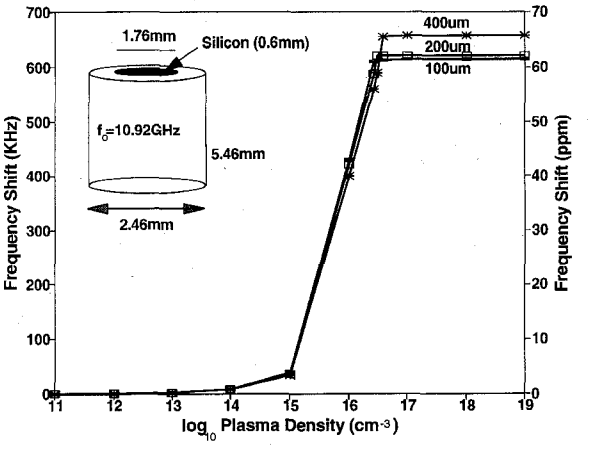

Fig. 4. Spectrum for a X-band resonator without a wafer (solid line), with a Si wafer (dashed line), and with GaAs wafer (dotted line).

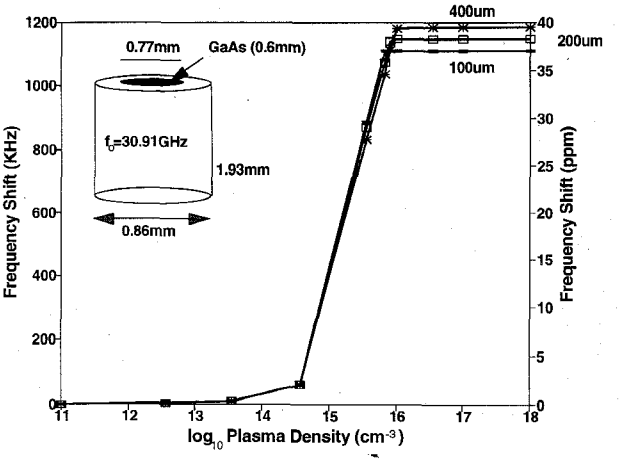

Fig. 5. Spectrum for an Si wafer tuned resonator without illumination (solid line), with illumination and $n_e = 10^{14}\,\mathrm{cm}^{-3}$ (dashed line), and with illumination and $n_e = 10^{18}\,\mathrm{cm}^{-3}$ (dotted line).

($D_s \times L_s = 0.77 \times 0.60\,\mathrm{mm}^2$) on a Ka-band ($f_0 = 30.91$ GHz) dielectric resonator ($D \times L = 1.93 \times 0.86\,\mathrm{mm}^2, \epsilon_r = 29.1$). No significant frequency shift occurs until a critical quantity of photoinduced plasma is created, after which it rises rapidly and saturates. Note that Δf is only weakly affected by the plasma thickness. This is expected, since the electrical skin depths at the resonator frequencies are less than the given plasma thickness. For these configurations, the relative maximum frequency shift for the X-band OCDR (70 ppm) is almost twice as great as that for the Ka-based OCDR (40 ppm).

The influence of the semiconductor on the X-band DR spectrum is shown in Fig. 4. A semiconductor layer strongly affects the high-order resonance modes, and both Si and GaAs have about the same effect on the fundamental mode. Fig. 5 shows the resonance frequency changes in an illuminated OCDR. As in the case of metal plate tuning, the resonator frequency goes up and the Q decreases as plasma density increases.

Fig. 6 shows the relationship between optical illumination irradiance and photoinduced plasma density. For a fixed pho-

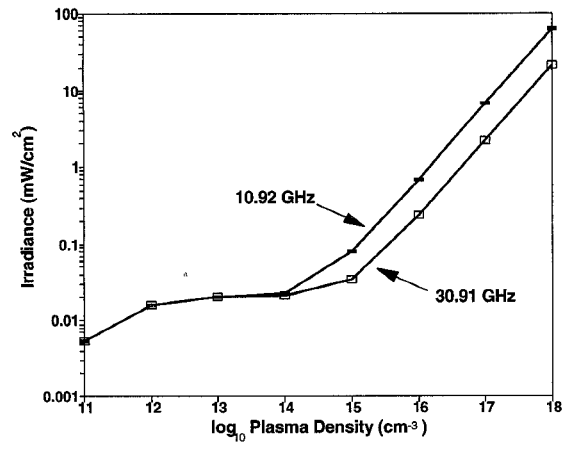

Fig. 6. Irradiance versus photoinduced carrier density ($T = 300$ K) for silicon wafer (solid line) and GaAs wafer (dashed line).

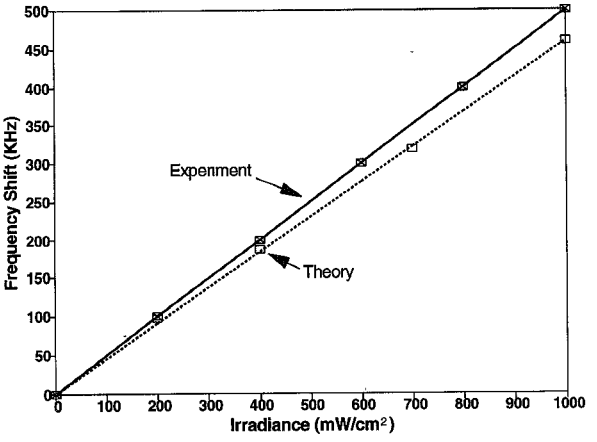

Fig. 7. Predicted shift in resonant frequency as a function of irradiance and experimental results of Herczfeld *et al.* [8].

toinduced plasma density and resonator tuning range, higher resonator frequencies require lower illumination irradiance.

B. Comparison with Experimental Results

The modified FDTD technique that we have developed was applied to an actual experiment by Herczfeld *et al.* [8] in an attempt to emulate their results. In the experiment, the $TE_{01\delta}$ mode frequency of an X-band DR was measured when overlaid with a Si slab. The plasma layer thickness and density was calculated from the parameters of Table II and the illumination reported in [8]. Our simulated results for a DR identical to that in [8] are compared with measurement in Fig. 7 and they are shown to agree within 8%. This result is encouraging, but it should be noted that the experimental material parameters were not available and not necessarily equal to the values in Table II.

IV. Conclusion

A frequency dependent form of the finite-difference time domain (FDTD) method has been developed for electromagnetic field calculations in materials which exhibit frequency dependent electrical constitutive parameters. This new technique lends itself to previously intractable problems of electromagnetic field simulations of optically induced solid state plasmas, allowing predictions of a host of two and three dimensional optically controlled microwave devices.

This paper describes the application of the $(FD)^2TD$ method to the simulation and determination of the resonance frequencies of an optically controlled dielectric resonator. Comparison of calculations to an experimental result shows fair agreement.

The authors intend on performing experiments to further test theoretical results and to apply the method to optically controlled microwave phase shifters. Also, this method can be used to analyze the active devices in MMIC circuits.

Acknowledgment

The authors wish to thank Prof. D. Conn, J. M. Zhang, Z. Bi, and C. Laperle of the Communications Research Laboratory of McMaster Unversity for several fruitful discussions, and acknowledge the seminal work of Prof. D. M. Xu of Shanghai University of Science and Technology. The authors also thank the reviewers who have significantly improved this paper through their helpful criticism.

References

[1] D. Kajfez and P. Guillon, *Dielectric Resonators.* Norwood, MA: Artech House, 1986.

[2] A. Karp, H. J. Shaw, and D. K. Winslow, "Circuit properties of microwave dielectric resonators," *IEEE Trans. Microwave Theory Tech.*, vol. MTT-16, pp. 818–828, Oct. 1968.

[3] J. R. Mahieu, "Low conversion up and down converters using dielectric resonators for applications with millimetre telecommunication systems," in *Proc. 6th European Microwave Conf.*, 1976, pp. 664–668.

[4] M. W. Pospieszalski, "Cylindrical dielectric resonators and their applications in TEM-line microwave circuits," *IEEE Trans. Microwave Theory Tech.*, vol. MTT-27, pp. 233–238, Feb. 1979.

[5] Y. Komatsu and Y. Murakami, "Coupling coefficient between microstrip line and dielectric resonator," *IEEE Trans. Microwave Theory Tech.*, vol. MTT-31, pp. 34–40, Jan. 1983.

[6] Y. Shen, Z. Bi, K. Wu, and J. Litva, "FD-TD analysis of open cylindrical dielectric resonators," *Microwve Opt. Tech. Lett.*, vol. 5, no. 6, pp. 261–265, June 1992.

[7] F. H. Gil and J. P. Martinez, "Analysis of dielectric resonators with tuning screw and supporting structure," *IEEE Trans. Microwave Theory Tech.*, vol. MTT-33, pp. 1453–1457, Dec. 1985.

[8] P. R. Herczfeld, A. Daryoush, C. D'Ascenzo, M. Contarino, and A. Rosen, "Optically controlled and FM modulated X-band dielectric resonator oscillator," in *Proc. 14th European Microwave Conf.*, 1984, pp. 268–273.

[9] A. J. Seeds and A. A. A. deSalles, "Optical control of microwave semiconductor devices," *IEEE Trans. Microwave Theory Tech.*, vol. MTT-38, pp. 577–585, May 1990.

[10] C. H. Lee, d"Picosecond optics and microwave technology," *IEEE Trans. Microwave Tech.*, vol. MTT-38, pp. 596–607, May 1990.

[11] M. A. Romero, A. L. A. Cunha, and A. A. A. deSalles, "Theory and experiment for HEMT's under optical illumination," in *1991 IEEE MTT-S Dig.*, pp. 495–498.

[12] A. Bangert and M. Ludwig, "A direct optical injection-locked 8 GHz MMIC oscillator," *1991 IEEE MTT-S Dig.*, pp. 499–502.

[13] C. H. Lee, P. S. Mak, and A. P. DeFonzo, "Optical control of millimeter-wave propagation in dielectric waveguides." *IEEE J.Quantum Elecron.*, vol. QE-16, pp. 277–288, Mar. 1980.

[14] P. C. D. P. Neikirk and T. Itoh, "Optically controlled coplanar waveguide phase shifters," *IEEE Trans. Microwave Theory Tech.*, vol. MTT-38, pp. 586–595, May 1990.

[15] K. S. Yee, "Numerical solution of initial boundary value problems involving Maxwell's equations in isotropic media," *IEEE Trans. Antennas Propagat.*, vol. AP-14, pp. 302–307, May 1966.

[16] J. C. Bolomey, C. Durix, and D. Lesselier, "Time domain integral equation approach for inhomogeneous and dispersive slab problems," *IEEE Trans. Antennas Propagat.,* vol. AP-26, pp. 658–667, Sept. 1978.
[17] R. J. Luebbers, F. P. Hunsberger, K. S. Kunz, R. B. Standler, and M. Schneider, "A frequency-dependent finite-difference time-domain formulation for dispersive materials," *IEEE Trans. Electromagn. Compat.,* vol. 32, pp. 222–227, Aug. 1990.
[18] R. J. Luebbers, F. P. Hunsberger, and K. S. Kunz, "A frequency-dependent finite-difference time-domain formulation for transient propagation in plasma," *IEEE Trans. Antennas Propagat.,* vol. AP-39, pp. 29–34, Jan. 1991.
[19] Z. Bi, Y. Shen, K. Wu, and J. Litva, "Fast finite-difference time-domain analysis of resonators using digital filtering and spectrum estimation techniques," *IEEE Trans. Microwave Theory Tech.,* vol. MTT-40, pp. 1611–1619, Aug. 1992.
[20] Y. Shen, Z. Bi, K. Wu, and J. Litva, "Efficient FD-TD analysis of dielectric resonators with tuning screw and miltilayer structures," in *1992 IEEE MTT-S Dig.,* pp. 967–970.
[21] R. A. Smith, *Semiconductors.* Cambridge, MA: Cambridge, 1968.
[22] R. F. Pierret, *Modular series on solid state devices, vol. VI: Advanced Semiconductor Fundamentals.* Reading, MA: Addison-Wesley, 1989.
[23] J. S. Blakemore, "Semiconducting and other major properties of gallium arsenide," *J. Appl. Phys.,* vol. 53, pp. R123–R181, Oct. 1982.
[24] Y. P. Varshni, "Band-to-band radiative recombination in groups IV, VI, and III-V semiconductors (I)," *Phys. Stat. Sol.,* vol. 19, pp. 459–514, 1967.
[25] Y. P. Varshni, "Band-to-band radiative recombination in groups IV, VI, and III-V semiconductors (II)," *Phys. Stat. Sol.,* vol. 20, pp. 9–36, 1967.

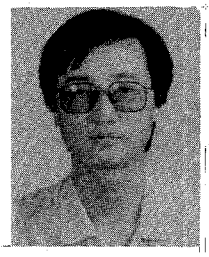

Ying Shen was born in Shanghai, China, on June 10, 1962. He received the B.S. and M.S. degrees from Shanghai University of Science and Technology, Shanghai, China, in 1984 and 1987, respectively.

From 1987 to 1988, he was a Teaching Assistant, and from 1988 to 1990 a Lecturer in the Radio-Electronics Department of Shanghai University of Science and Technology, Shanghai. Since 1991 he has been a Teaching Assistant in the Department of Electrical and Computer Engineering at McMaster University, where he is working toward the Ph.D. degree. His current research interests include the design of microwave monolithic integrated circuits, integrated active antennas, the FDTD method for analyzing MIC and MMIC components, and the interaction of microwave and optics.

Kent Nickerson received the B.Sc. degree in physics from the University of Waterloo in 1981. Becoming a self-taught electronics designer through personal experimentation in music synthesis, he was employed as an engineer in industry before coming to McMaster University. There he received the M.Eng. degree, with distinction, in electrical engineering in 1986, serving a term as a special lecturer in the department.

As a Research Engineer at the Communications Research Laboratory of McMaster University, he studies the optical control of microwave devices and is presently developing an electrooptic sampling system for microwave measurements.

Mr. Nickerson is a member of SPIE.

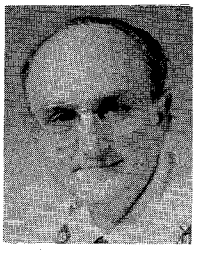

John Litva (SM'92) is currently a Professor in Electrical Engineering at McMaster University, Hamilton, Ont., Canada, and an External Professor at the East China Institute of Technology in Nanjing, China. He is the holder of the Microwave Antenna Chair sponsored by Spar Aerospace, Andrew Canada, and NSERC, as well as being a Thrust Leader in the Telecommunications Institute of Ontario (TRIO). TRIO is a university-industry based Center of Excellence, which is funded by the province of Ontario, and whose mandate is to conduct research in support of the telecommunications industry in Ontario. Prior to 1985, he was a Research Scientist with the Radar Laboratory, Communications Research Center, Ottawa, where his primary area of research was digital beamforming, array antennas, and signal processing. He has lectured in Nanjing, Shanghai, and Beijing, China, on selected topics in numerical techniques for analyzing microstrip antennas, digital, nonlinear and adaptive beamforming, integrated antennas, and simulation and analyses of multipath signals. At present his interests are centered on 1) digital beamforming for satellite communications, 2) phased array antenna theory, 3) numerical analysis of antennas and microwave devices, 4) integrated antennas, 5) radio-wave direction finding, and 6) nonlinear and adaptive beamforming.